Journal of Naval Architecture and Marine Engineering
December, 2011
DOI: 10.3329/jname.v8i2.7392 http://www.banglajol.info

INFLUENCE OF CENTERED CONDUCTING OBSTACLE ON MHD COMBINED CONVECTION IN A WAVY CHAMBER

Rehena Nasrin

Department of Mathematics, Bangladesh University of Engineering and Technology, Dhaka-1000, Bangladesh.

Email: rehena@math.buet.ac.bd

Abstract:

The development of centered heat conducting obstacle effect on combined magnetoconvective flow in a lid driven chamber has been numerically studied. The enclosure considered has rectangular horizontal lower surfaces and vertical side surfaces. The lower and upper surfaces are insulated. The left wall is mechanically lid driven having uniform temperature T_i and velocity v_0 while other vertical side is wavy and maintains higher temperature T_h than the lid. The governing two-dimensional flow equations have been solved by using Galerkin weighted residual finite element technique. The investigations are conducted for different values of Richardson number (Ri) and physical parameter i.e. diameter (D) of square solid body. Various characteristics such as streamlines, isotherms and heat transfer rate in terms of the mean Nusselt number (Nu), the average temperature (θ_{av}) of the fluid and temperature of obstacle center (θ_c) are presented. The results indicate that the mentioned parameters strongly affect the flow phenomenon and temperature field inside the chamber. Conducting largest obstacle is preferable for effective heat transfer mechanism in presence of magnetic field.

Keywords: Combined convection, MHD, wavy chamber, heat conducting obstacle, finite element simulation.

NOMENCLATURE

A	amplitude of wavy surface
B_0	magnetic field strength (Wbm^{-2})
C_p	specific heat at constant pressure ($JKg^{-1}K^{-1}$)
d	dimensional size of the conducting body (m)
D	non-dimensional size of the solid body
g	acceleration due to gravity (ms^{-2})
h	convective heat transfer coefficient ($Wm^{-2}K^{-1}$)
Ha	Hartmann number
K	solid-fluid thermal conductivity ratio
k	thermal conductivity of fluid ($Wm^{-1}K^{-1}$)
L	length of the cavity (m)
Nu	Nusselt number
p	dimensional pressure (Nm^{-2})
P	non-dimensional pressure
Pr	Prandtl number
Ra	Rayleigh number
Re	Reynolds number
Ri	Richardson number
v_0	lid velocity (ms^{-1})
$\overline{V}$	cavity volume (m^3)
T	dimensional temperature of fluid (K)
ΔT	dimensional temperature difference (K)
u, v	velocity components (ms^{-1})
U, V	non-dimensional velocity components

Greek symbols

α	thermal diffusivity (m^2s^{-1})
β	thermal expansion coefficient (K^{-1})
θ	non-dimensional temperature
λ	number of undulations
μ	dynamic viscosity of the fluid ($Kg\ m^{-1}s^{-1}$)
ν	kinematic viscosity of the fluid (m^2s^{-1})
ρ	density of the fluid ($Kg\ m^{-3}$)
σ	electrical conductivity of the fluid ($\Omega^{-1}m^{-1}$)

Subscripts

av	average
c	centre
h	heated wavy wall
i	less heated lid
s	solid
x, y	Cartesian coordinates (m)
X, Y	non-dimensional Cartesian coordinates

1813-8235 (Print), 2070-8998 (Online) Received on: April 2011

1. Introduction

The influence of the magnetic field on the convective heat transfer and the mixed convection flow of the fluid are of paramount importance in engineering. A combined free and forced convection flow of an electrically conducting fluid in a cavity or in a channel in the presence of magnetic field is of special technical significance because of its frequent occurrence in many industrial applications such as geothermal reservoirs, cooling of nuclear reactors, thermal insulations and petroleum reservoirs. These types of problems also arise in electronic packages, micro electronic devices during their operations.

Papanicolaou and Jaluria (1990) carried out a numerical study to investigate the combined forced and natural convective cooling of heat dissipating electronic components, located in rectangular enclosure and cooled by an external flow of air. At the same year, House et al. (1990) considered natural convection in a vertical square cavity with heat conducting body, placed on center in order to understand the effect of the heat conducting body on the heat transfer process in the cavity. They found that the heat transfer across the enclosure enhanced by a body with thermal conductivity ratio less than unity. Garandet et al. (1992) studied natural convection heat transfer in a rectangular enclosure with a transverse magnetic field. Rudraiah et al. (1995) investigated the effect of surface tension on buoyancy driven flow of an electrically conducting fluid in a rectangular cavity in the presence of a vertical transverse magnetic field to see how this force damped hydrodynamic movements. Calmidi and Mahajan (1998) studied mixed convection in a partially divided rectangular enclosure over a wide range of Reynolds and Grashof numbers. Their findings were that the average Nusselt number and the dimensionless surface temperature depended on the location and height of the divider.

Combined free and forced convection in a square enclosure with heat conducting body and a finite-size heat source was simulated numerically by Hsu and How (1999). They concluded that both the heat transfer coefficient and the dimensionless temperature in the body center strongly depended on the configurations of the system. At the same time, Omri and Nasrallah (1999) studied mixed convection in an air-cooled cavity with differentially heated vertical isothermal sidewalls having inlet and exit ports by a control volume finite element method. Results showed two different placement configurations of the inlet and exit ports on the sidewalls. Best configuration was selected analyzing the cooling effectiveness of the cavity, which suggested that injecting air through the cold wall was more effective in heat removal and placing inlet near the bottom and exit near the top produced effective cooling. The problem of unsteady laminar combined forced and free convection flow and heat transfer of an electrically conducting and heat generating or absorbing fluid in a vertical lid-driven cavity in the presence of magnetic field was formulated by Chamkha (2002).

Shokouhmand and Sayehvand (2004) carried out the numerical study of flow and heat transfer in a square driven cavity. They found that at the higher values of Reynolds number, an inviscid core region developed, but secondary eddies were present in the bottom corners of the square at all Reynolds numbers. Bhoite et al. (2005) conducted numerically the problem of mixed convection flow and heat transfer in a shallow enclosure with a series of block-like heat generating component for a range of Reynolds and Grashof numbers and block-to-fluid thermal conductivity ratios. The authors declared that higher Reynolds number created a recirculation region of increasing strength at the core region and the effect of buoyancy became insignificant beyond a Reynolds number of typically 600, and the thermal conductivity ratio had a negligible effect on the velocity fields. Al-Amiri et al. (2007) performed mixed convection heat transfer in lid-driven cavity with a sinusoidal wavy bottom surface, where the corrugated lid-driven cavity could be considered as an effective heat transfer mechanism at larger wavy surface amplitudes and low Richardson number.

Recently, Oztop et al. (2009) analyzed fluid flow due to combined convection in lid-driven enclosure having a circular body. Mixed convection in an obstructed open-ended cavity with heated horizontal walls was analyzed by Shi and Vafai (2010). They declared that the vertical velocity component was substantially diminished within a narrow entrance section near the inlet boundary for an inclined flow. As the aspect ratio increased the thickness of the thermal boundary layer increased, resulted in a decrease in the heat transfer rate though the horizontal walls. Very recently, mixed convection in a square cavity of sinusoidal boundary conditions at the sidewalls in the presence of magnetic field was investigated numerically by Sivasankaran et al. (2011). They concluded that the heat transfer rate increased with the phase deviation up to $\phi = \pi/2$ and then it decreased for further increase in the phase deviation. Also it increased on increasing the amplitude ratio. At the same year, Nasrin and Parvin (2011) thoroughly studied hydromagnetic effect on mixed convection in a lid-driven cavity with sinusoidal corrugated bottom surface, where the average Nusselt number at the heated surface increased with an increase of the number of waves as well as the Reynolds number, while decreased with increasing Hartmann number.

In the light of the above literature, it has been pointed out that there is no significant information about effect of heat conducting obstacle on the combined convection processes in a wavy chamber. The present study addresses this issue. Numerical solutions are obtained over a wide range of *Ri* and *D*. Results are presented graphically in terms of streamlines and isothermal lines. Finally the average Nusselt number at the heated surface, the mean temperature of the fluid and the temperature of solid body center are calculated.

2. Problem Formulation

The geometry of the problem with necessary boundary conditions herein investigated is depicted in Fig. 1. The system consists of a two-dimensional lid driven square chamber of length *L*. The base and top part of the cavity are well insulated. It is assumed that the left lid is at a uniform velocity v_0 and at the temperature T_i. As well the right vertical corrugated wall is more heated than the left lid with the temperature T_h. A square heat conducting obstacle is centered of the chamber. The functioning fluid is assumed as air (Pr = 0.73). A magnetic field of strength B_0 is applied in the transverse direction to the side walls of the cavity.

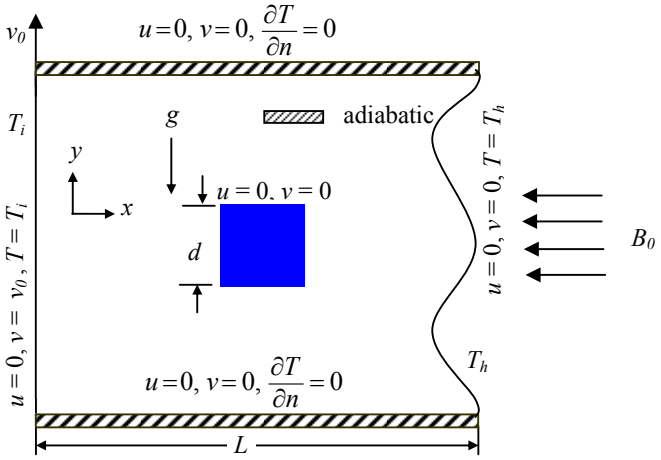

Fig. 1: Schematic diagram of the chamber and boundary conditions

3. Mathematical Formulation

A two-dimensional, steady, laminar, incompressible, mixed convection flow is considered within the chamber and the fluid properties are assumed to be constant. The radiation effect is taken as negligible. The dimensional equations describing the flow under Boussinesq approximation are as follows:

$$\frac{\partial u}{\partial x}+\frac{\partial v}{\partial y}=0 \tag{1}$$

$$u\frac{\partial u}{\partial x}+v\frac{\partial u}{\partial y}=-\frac{1}{\rho}\frac{\partial p}{\partial x}+\nu\left(\frac{\partial^2 u}{\partial x^2}+\frac{\partial^2 u}{\partial y^2}\right) \tag{2}$$

$$u\frac{\partial v}{\partial x}+v\frac{\partial v}{\partial y}=-\frac{1}{\rho}\frac{\partial p}{\partial y}+\nu\left(\frac{\partial^2 v}{\partial x^2}+\frac{\partial^2 v}{\partial y^2}\right)+g\beta\left(T-T_i\right)-\frac{\sigma {B_0}^2 v}{\rho} \tag{3}$$

$$u\frac{\partial T}{\partial x}+v\frac{\partial T}{\partial y}=\frac{k}{\rho c_p}\left(\frac{\partial^2 T}{\partial x^2}+\frac{\partial^2 T}{\partial y^2}\right) \tag{4}$$

$$\frac{k_s}{\rho c_p}\left(\frac{\partial^2 T_s}{\partial x^2}+\frac{\partial^2 T_s}{\partial y^2}\right)=0 \tag{5}$$

The boundary conditions for the present phenomena are specified as follows:

at the vertical lid: $u=0, v=v_0,\ T=T_i$

at the horizontal walls: $u = 0, v = 0, \dfrac{\partial T}{\partial n} = 0$

at the wavy surface: $u = 0, v = 0, T = T_h$

at all cylinder boundaries: $u = 0, v = 0$

at the solid-fluid interface: $\left(\dfrac{\partial T}{\partial n}\right)_{fluid} = \dfrac{k_s}{k}\left(\dfrac{\partial T_s}{\partial n}\right)_{solid}$

The rate of heat transfer is computed at the wavy wall and is expressed in terms of the local Nusselt number $\overline{Nu}$ as $\overline{Nu} = \dfrac{hL}{k} = -\dfrac{\partial T}{\partial n}L$

where h and n is the local convective heat transfer coefficient and dimensional distances either along x or y direction acting normal to the surface.

The above equations are non-dimensionalized by using the following dimensionless quantities

$$X = \frac{x}{L}, \quad Y = \frac{y}{L}, \quad U = \frac{u}{v_0}, \quad V = \frac{v}{v_0}, \; D = \frac{d}{L}, P = \frac{p}{\rho\, {v_0}^2}, \theta = \frac{(T - T_i)}{(T_h - T_i)}, \; \theta_s = \frac{(T_s - T_i)}{(T_h - T_i)}$$

Then the non-dimensional governing equations are

$$\frac{\partial U}{\partial X} + \frac{\partial V}{\partial Y} = 0 \tag{6}$$

$$U\frac{\partial U}{\partial X} + V\frac{\partial U}{\partial Y} = -\frac{\partial P}{\partial X} + \frac{1}{Re}\left(\frac{\partial^2 U}{\partial X^2} + \frac{\partial^2 U}{\partial Y^2}\right) \tag{7}$$

$$U\frac{\partial V}{\partial X} + V\frac{\partial V}{\partial Y} = -\frac{\partial P}{\partial Y} + \frac{1}{Re}\left(\frac{\partial^2 V}{\partial X^2} + \frac{\partial^2 V}{\partial Y^2}\right) + Ri\,\theta - \frac{Ha^2}{Re}V \tag{8}$$

$$U\frac{\partial \theta}{\partial X} + V\frac{\partial \theta}{\partial Y} = \frac{1}{RePr}\left(\frac{\partial^2 \theta}{\partial X^2} + \frac{\partial^2 \theta}{\partial Y^2}\right) \tag{9}$$

$$\frac{K}{RePr}\left(\frac{\partial^2 \theta_s}{\partial X^2} + \frac{\partial^2 \theta_s}{\partial Y^2}\right) = 0 \tag{10}$$

where $Re = \dfrac{v_0 L}{\nu}$, $Pr = \dfrac{\nu}{\alpha}$, $Ra = \dfrac{g\beta(T_h - T_i)L^3}{\nu\alpha}$ and $Ri = \dfrac{Ra}{Re^2\, Pr}$ are Reynolds number, Prandtl number, Rayleigh number and Richardson number respectively and Ha is Hartmann number which is defined as $Ha^2 = \dfrac{\sigma B_0^2 L^2}{\mu}$.

The boundary conditions for the current problem are specified as follows:

at the left lid: $U = 0$, $V = 1$, $\theta = 0$

at the horizontal surfaces: $U = 0$, $V = 0$, $\dfrac{\partial \theta}{\partial N} = 0$

at the wavy wall: $U = V = 0$, $\theta = 1$

at the solid boundary: $U = V = 0$

at the fluid-solid interface: $\left(\dfrac{\partial \theta}{\partial N}\right)_{fluid} = K\left(\dfrac{\partial \theta_s}{\partial N}\right)_{solid}$

where N is the non-dimensional distances either X or Y direction acting normal to the surface and K is ratio of the thermal conductivity (k_s / k).

The nature of the vertical wavy surface profile is assumed the pattern of $X - 1 = -A[1 - \cos(2\lambda\pi Y)]$, where A is the dimensionless amplitude of the corrugated surface and λ is the number of undulations.

The local Nusselt number at the heated corrugated surface is $\overline{Nu} = -\frac{\partial\theta}{\partial N} L$.

The normal temperature gradient can be written as

$$\frac{\partial\theta}{\partial N} = \frac{1}{L}\sqrt{\left(\frac{\partial\theta}{\partial X}\right)^2 + \left(\frac{\partial\theta}{\partial Y}\right)^2}$$

while the average Nusselt number (Nu) is obtained by integrating the local Nusselt number along the vertical wavy surface and is defined by

$$Nu = \frac{1}{S}\int_0^S \overline{Nu}\ \ dN$$

where S is the dimensionless chord length of the wavy surface.

The mean temperature of the fluid is $\theta_{av} = \int \theta\, d\overline{V} / \overline{V}$, where $\overline{V}$ is the volume of the chamber.

4. Finite Element Simulation

The momentum and energy balance equations are the combinations of mixed elliptic-parabolic system of partial differential equations. These equations have been solved by using the Galerkin weighted residual finite element technique of Rahman et al. (2010). Due to mass conservation, the continuity equation has been used as a constraint. The velocity components U and V, the temperature θ and the pressure P are the basic unknowns in the above differential equations. The six node triangular element is used in this work for the development of the finite element equations. All six nodes are associated with velocities as well as temperature. Only the three corner nodes are associated with pressure. This means that a lower order polynomial is chosen for pressure and which is satisfied through continuity equation. The velocity components, the temperature distribution and linear interpolation for the pressure distribution according to their highest derivative orders in the differential equations (6) - (10) are as follows

$$U(X,Y) = N_\beta U_\beta,\ V(X,Y) = N_\beta V_\beta,\ \theta(X,Y) = N_\beta \theta_\beta,\ \theta_s(X,Y) = N_\beta \theta_{s_\beta},\ P(X,Y) = H_\lambda P_\lambda,$$

where $\beta = 1, 2, \ldots\ldots, 6$ and $\lambda = 1, 2, 3$.

The finite element equations can be modified in the form given below by substituting the element velocity components, the temperature and the pressure distributions in the equations (6) - (10)

$$K_{\alpha\beta\gamma^x} U_\beta U_\gamma + K_{\alpha\beta\gamma^y} V_\gamma U_\gamma + M_{\alpha\mu^x} P_\mu + \frac{1}{Re}\left(S_{\alpha\beta^{xx}} + S_{\alpha\beta^{yy}}\right) U_\beta = Q_{\alpha^u} \tag{11}$$

$$K_{\alpha\beta\gamma^x} U_\beta V_\gamma + K_{\alpha\beta\gamma^y} V_\gamma V_\gamma + M_{\alpha\mu^y} P_\mu + \frac{1}{Re}\left(S_{\alpha\beta^{xx}} + S_{\alpha\beta^{yy}}\right) V_\beta - Ri\, K_{\alpha\beta}\theta_\beta + \frac{Ha^2}{Re} K_{\alpha\beta} V_\beta = Q_{\alpha^v} \tag{12}$$

$$K_{\alpha\beta\gamma^x} U_\beta \theta_\gamma + K_{\alpha\beta\gamma^y} V_\beta \theta_\gamma + \frac{1}{Re\, Pr}\left(S_{\alpha\beta^{xx}} + S_{\alpha\beta^{yy}}\right)\theta_\beta = Q_{\alpha^\theta} \tag{13}$$

$$\frac{K}{Re\, Pr}\left(S_{\alpha\beta^{xx}} + S_{\alpha\beta^{yy}}\right)\theta_\beta = Q_{\alpha^{\theta_s}} \tag{14}$$

where the coefficients in element matrices are in the form of the integrals over the element area and along the element edges S_0 and S_w as

$$K_{\alpha\beta^x} = \int_A N_\alpha N_{\beta,x} dA, \quad K_{\alpha\beta^y} = \int_A N_\alpha N_{\beta,y} dA, \quad K_{\alpha\beta\gamma^x} = \int_A N_\alpha N_\beta N_{\gamma,x} dA, \quad K_{\alpha\beta\gamma^y} = \int_A N_\alpha N_\beta N_{\gamma,y} dA,$$

$$K_{\alpha\beta} = \int_A N_\alpha N_\beta dA, \quad S_{\alpha\beta^{xx}} = \int_A N_{\alpha,x} N_{\beta,x} dA, \quad S_{\alpha\beta^{yy}} = \int_A N_{\alpha,y} N_{\beta,y} dA, \quad M_{\alpha\mu^x} = \int_A H_\alpha H_{\mu,x} dA,$$

$$M_{\alpha\mu^y} = \int_A H_\alpha H_{\mu,y} dA, \quad Q_{\alpha^u} = \int_{S_0} N_\alpha S_x dS_0, \quad Q_{\alpha^v} = \int_{S_0} N_\alpha S_y dS_0, \quad Q_{\alpha\theta} = \int_{S_w} N_\alpha \, q_{1w} dS_w,$$

$$Q_{\alpha\theta_s} = \int_{S_w} N_\alpha \, q_{2w} dS_w$$

Using Newton-Raphson method of Reddy (1993), the set of non-linear algebraic equations (11) - (14) are transferred into linear algebraic equations. Finally, these linear equations are solved by applying Triangular Factorization method and reduced integration technique of Zeinkiewicz et al. (1971).

4.1 Grid Refinement Test

A grid independence test is reported with Ha = 12, Re = 100, K = 7, A = 0.05, D = 0.2, λ = 2, Ri = 0.1 and Pr = 0.73 in order to decide the suitable grid size for this study. The following five kinds of meshes are considered for the grid sensitivity investigation. These grid densities are 3918 nodes, 436 elements; 9373 nodes, 1064 elements; 15465 nodes, 1768 elements; 31514 nodes, 3636 elements and 49592 nodes, 5748 elements. The extreme values of the mean Nusselt number (Nu) that relates to the heat transfer rate of the heated surface and average temperature (θ_{av}) of the fluid in the chamber are used as sensitivity measures of the correctness of the solution. They are selected as the supervising variables for the grid liberty test. The addiction of the quantities Nu and θ_{av} on the grid size and the computational time are shown in Table 1. Considering both the accuracy of numerical values and computational time, the current formulation is performed with 31514 nodes and 3636 elements grid system.

Table 1. Grid Sensitivity Check at Ha = 12, Pr = 0.73, Ri = 0.1, Re = 100, A = 0.05, K = 7, λ = 2 and D = 0.2

Nodes (elements)	3918 (436)	9373 (1064)	15465 (1768)	31514 (3636)	49592 (5748)
Nu	1.597893	1.602778	1.618247	1.622647	1.622647
θ_{av}	0.336241	0.325121	0.310542	0.306112	0.306112
Time (s)	246.269	308.603	398.167	445.321	550.379

4.2 Mesh Generation

In finite element method, the mesh generation is the technique to subdivide a domain into a set of sub-domains, called finite elements, control volume etc. The discrete locations are defined by the numerical grid, at which the variables are to be calculated. It is basically a discrete representation of the geometric domain on which the problem is to be solved. The computational domains with irregular geometries by a collection of finite elements make the method a valuable practical tool for the solution of boundary value problems arising in various fields of engineering. Fig. 2 displays the finite element mesh of the present physical domain.

4.3 Code Validation

The model validation is a necessary part of a mathematical investigation. Hence, the outcome of the present numerical code is benchmarked against the numerical result of Rahman and Alim (2010) which was reported for MHD mixed convection flow in a vertical lid-driven square enclosure including a heat conducting horizontal circular cylinder with Joule heating. The comparison is conducted while employing the dimensionless parameters Re = 100, Ri = 5.0, K = 5.0, Ha = 10.0, J = 1.0, D = 0.2 and Pr = 0.71. Present result for both the streamlines and isotherms is shown in Fig. 3, which is an outstanding agreement with those of Rahman and Alim (2010). This justification boosts the assurance in this numerical code to carry on with the above stated objective of the existing investigation.

5. Results and Discussion

A numerical computation has been carried out through finite element simulation to analyze the effect of heat conducting obstacle on magnetohydrodynamic (MHD) mixed convection in a horizontal wavy chamber. Effects

of the controlling parameters such as Richardson number and diameter of the square obstacle on heat transfer and fluid flow inside the cavity have been studied. The changes in flow and temperature fields in terms of streamlines and isotherms, average Nusselt number, mean fluid temperature and temperature of solid center are focused in the following section. The ranges of *Ri* and *D* for this investigation vary from 0.1 to 10 and 0 to 0.5 respectively while the Prandtl number *Pr* (= 0.73), Hartmann number *Ha* (= 12), Reynolds number *Re* (= 100) and thermal conductivity ratio *K* (= 7) kept as invariable.

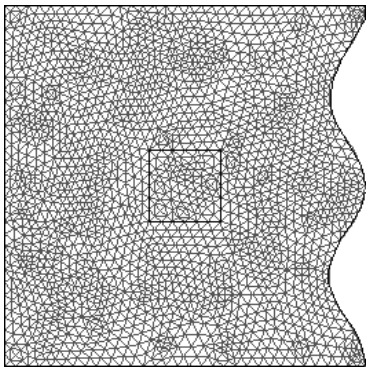

Fig. 2: Mesh structure of elements for wavy enclosure with a centered conducting obstacle

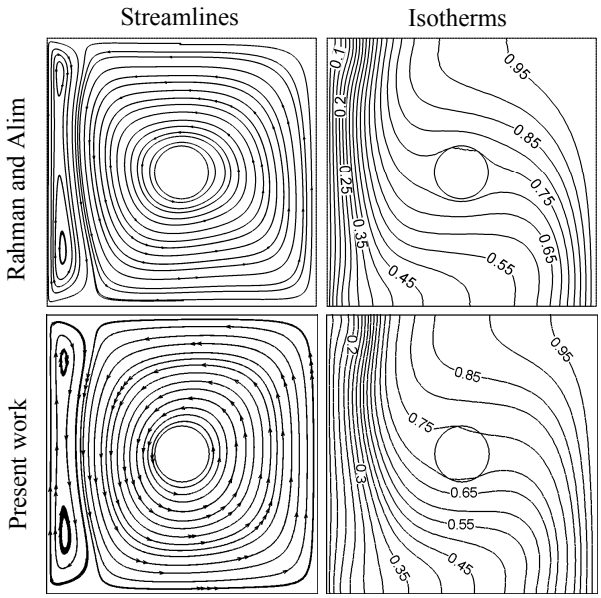

Fig. 3: Comparison between present work and Rahman and Alim (2010) using *Re* = 100, *Ri* = 5.0, *K* = 5.0, *Ha* = 10.0, *J* = 1.0, *D* = 0.2 and *Pr* = 0.71

The influence of physical parameter *D* (= 0, 0.2, 0.35, 0.5) on streamlines as well as isotherms for the present configuration at *Ri* = 0.1 with *Ha* = 12, *K* = 7 and *Pr* = 0.73 has been demonstrated in Fig. 4(a) - (b). The flow with the absence of heat conducting obstacle (*D* = 0) creates a clockwise circulation cell. By the forced convection effect the mechanically driven lid generates this circulatory behavior of velocity field. In the presence of this cylinder with rising diameters, there is insignificant change in the streamlines. But the shape and location of the center modify radically of the circulatory flow. Corresponding temperature field shows that in the absence of solid body the isothermal lines near the corrugated wall are parallel to the heated surface and parabolic shape isotherms are seen at the left top corner in the cavity. They start to gather in the vicinity of the left lid with growing obstacle diameter forming a thin thermal boundary layer.

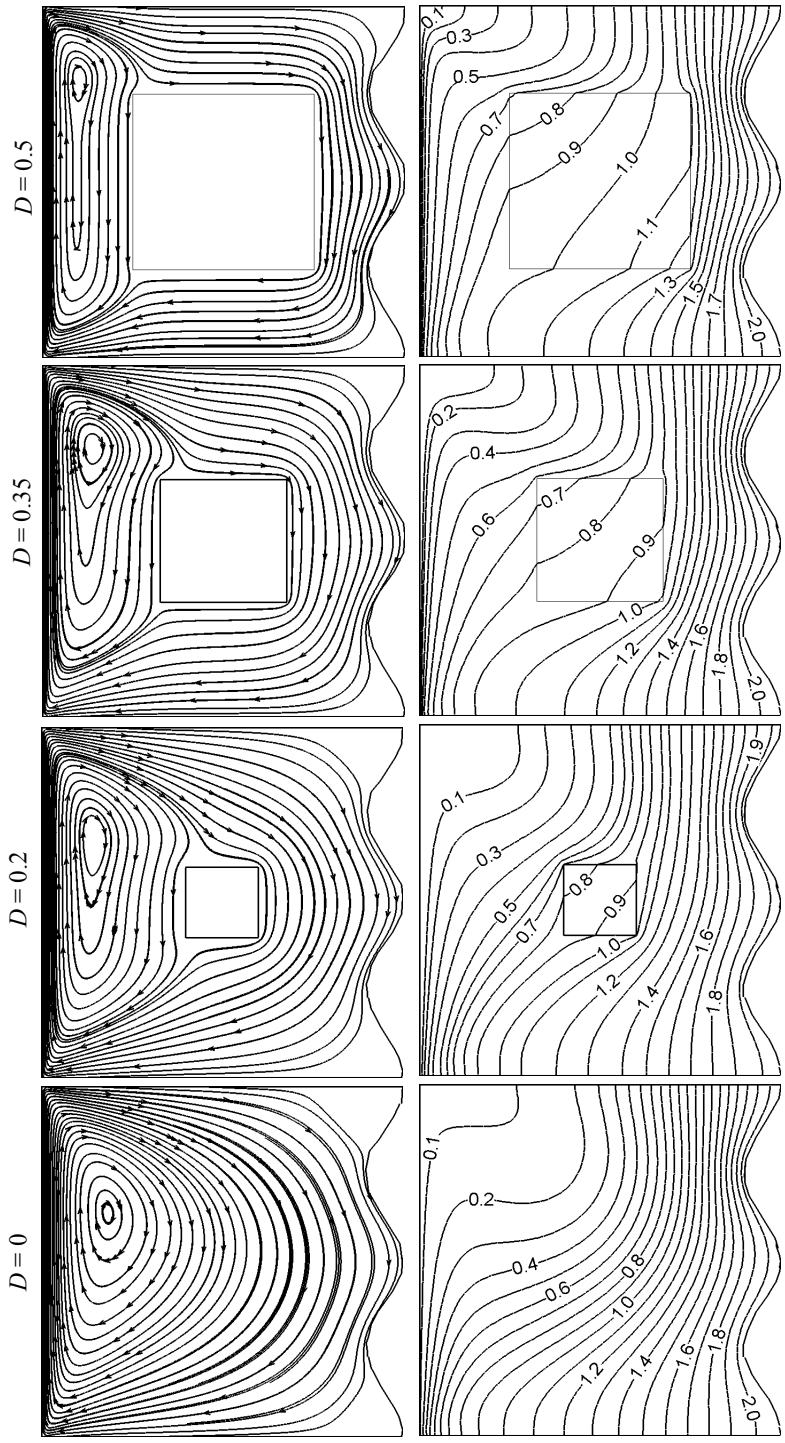

Fig. 4**:** Effect of *D* with *Ri* = 0.1 on (a) Streamlines and (b) Isotherms, while *Re* = 100, *Pr* = 0.73, *K* = 7 and *Ha* = 12.

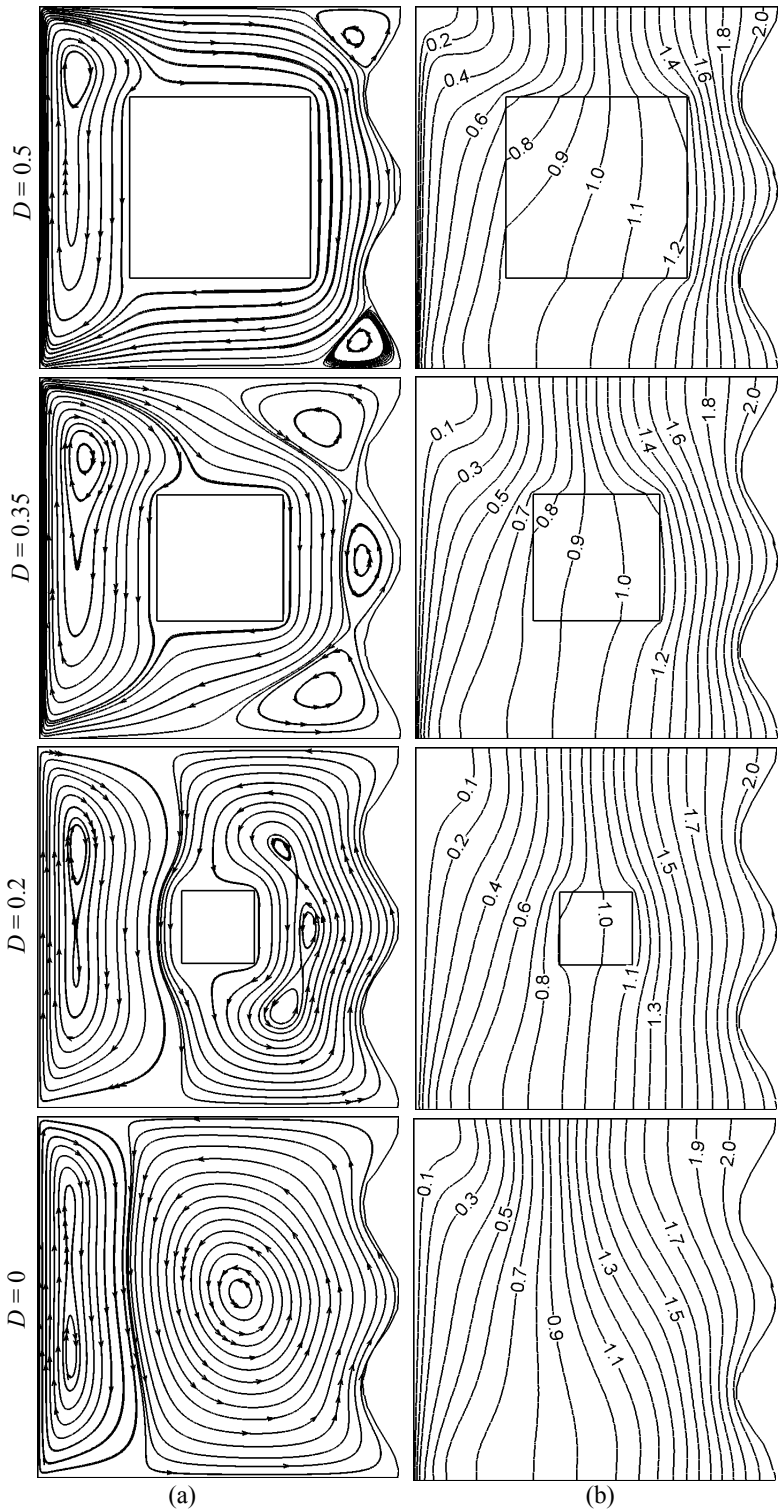

Fig. 5**:** Effect of D with Ri = 1 on (a) Streamlines and (b) Isotherms, while Re = 100, Pr = 0.73, K = 7 and Ha = 12.

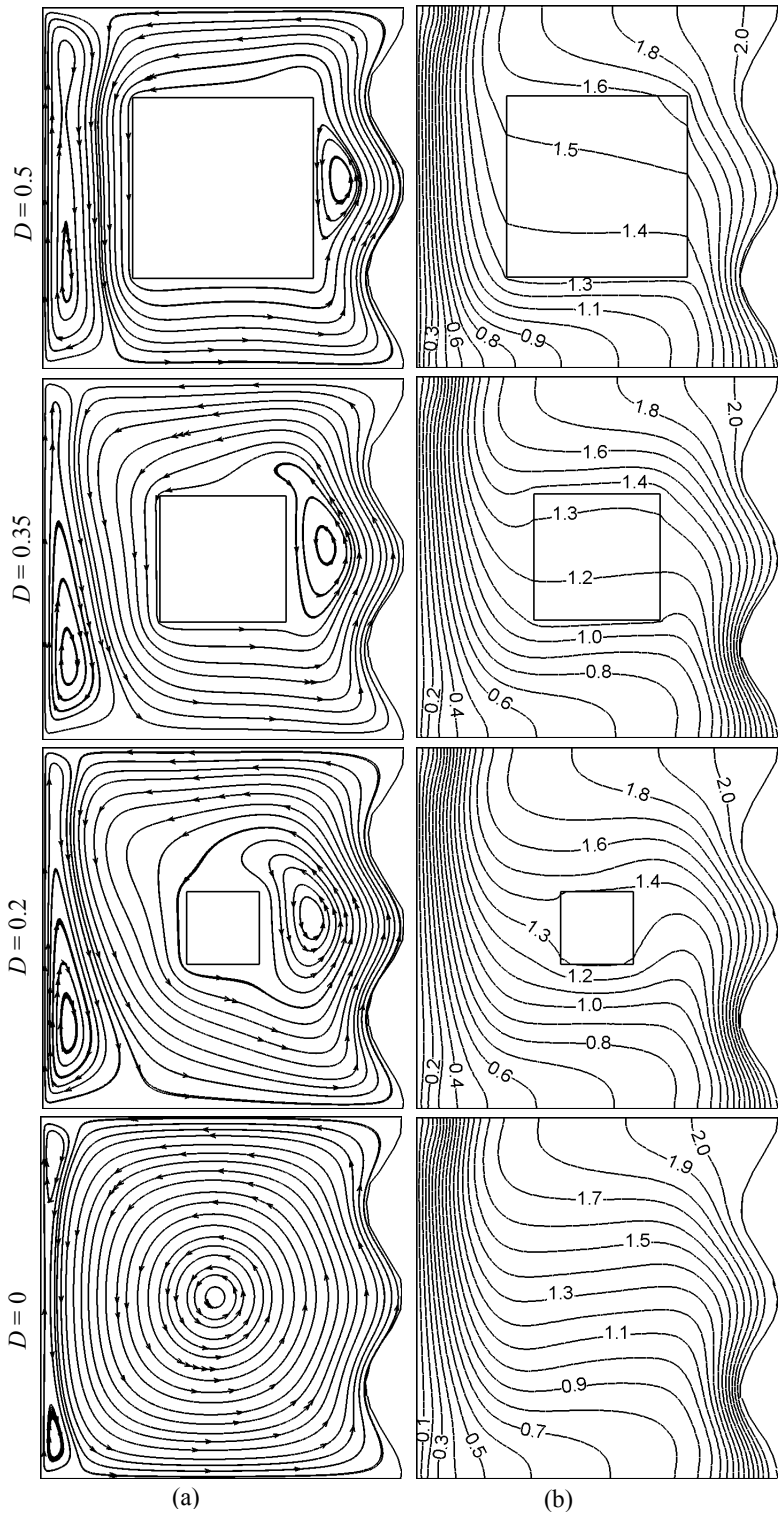

(a) (b)

Fig. 6**:** Effect of D with Ri = 10 on (a) Streamlines and (b) Isotherms, while Re = 100, Pr = 0.73, K = 7 and Ha = 12.

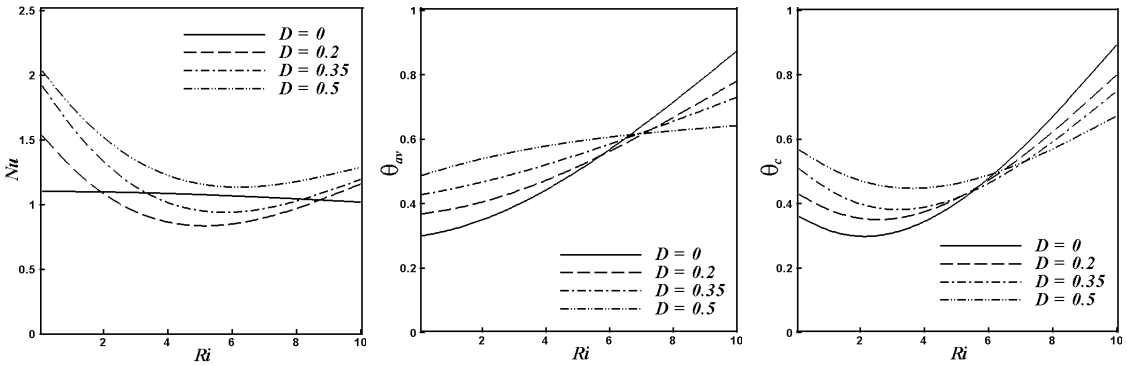

(a) (b) (c)

Fig. 7: Effect of diameter on (i) mean Nusselt number, (ii) average fluid temperature and (iii) temperature at the solid center while Re = 100, Ha = 12, Pr = 0.73 and K = 7

Fig. 5(a) - (b) expresses the flow and temperature field for different D at Ri = 1 while Pr = 0.73, K = 7. Ha = 12 and Re = 100. In the flow domain two counter rotating cells become visible. This is formal due to combined convection property. The lid driven wall generates the clockwise revolving cell whereas other one is created by the buoyancy force for the case of no obstacle. In the presence of obstacle with D (= 0.2 and 0.35), larger unicellular anticlockwise rotating cell becomes tri-cellular and smaller, consequently other one becomes bigger than previous case (no obstacle). At D = 0.5, two small vortices develop at the top and bottom corner near the wavy surface, because the larger obstacle reduces the available area for the buoyancy-induced recirculation. On the other hand, the isotherms take the wavy pattern in the cavity. The thermal current activities become analogous due to the variation of D.

The changes in fluid flow and isotherm patterns at Ri = 10 (buoyancy dominated regime) for various diameter of heat conducting body have been depicted in Fig. 6(a) - (b). A large anti-clockwise whirling cell in the fluid motion occupying almost the whole cavity is seen for all cases while the cell becomes more strengthen as D devalues. The change in temperature profile for mounting values of D is remarkable. The isothermal lines are linear and parallel near the less heated surface as shown in Fig. 6(b). They become bending at the mid position in the cavity, which is owing to the strong influence of the convective current in the cavity. The thermal boundary layer thickness near the lower part of hot wavy wall reduces as D grows up.

Variation of the mean Nusselt number, the average bulk temperature of the fluid and the temperature at the obstacle center for governing parameters D and Ri are shown in Fig. 7(a) – (c). For the higher values of D (D = 0.2, 0.35 and 0.5), Nu decreases very quickly in the mixed convection region and increases gradually in the free convection dominated region. On the other hand, in the absence of heat conducting obstacle, the average Nusselt number devalues mildly with increasing Ri. At the highest D, maximum average Nusselt number is always found. Fig. 7(b) – (c) shows that average temperature (θ_{av}) of the fluid in the chamber and temperature at the obstacle center are in similar pattern. That is, they increase with increasing physical parameter D at Ri = 0.1 whereas these quantities decrease at Ri = 10.

6. Conclusion

A computational study is performed to analysis the effect of heat conducting obstacle on combined convection in a vertical lid driven chamber in presence of magnetic field. The following outcomes can be written from the foregoing study

- The influence of diameter on streamlines and isotherms are remarkable at Ri = 0.1 and 10 respectively. Tiny eddies arise in top and bottom wavy corner and the isotherms take the wavy pattern for Ri = 1 with growing values of D.
- The combined convection parameter Ri has significant effects on the flow and temperature fields. Different types of flow and thermal current activities are observed at different convection region.
- The mean Nusselt number is optimum for the largest value of D. Thus, conducting largest obstacle is preferable for effective heat transfer mechanism.

- In the absence of solid obstacle and for $D = 0.5$, the average temperature of the fluid becomes lesser in the forced and free convection dominated regions respectively.
- The similar outcome is obtained for temperature at the obstacle center in the chamber.

References

Al-Amiri, A., Khanafer, K., Bull, J., Pop, Ioan (2007): Effect of sinusoidal wavy bottom surface on mixed convection heat transfer in a lid-driven cavity, International Journal of Heat and Mass Transfer, Vol. 50, No. (9–10), pp. 1771–1780. doi:10.1016/j.ijheatmasstransfer.2006.10.008

Bhoite, M. T., Narasimham, G. S. V. L., Murthy, M. V. K (2005): Mixed convection in a shallow enclosure with a series of heat generating components, International Journal of Thermal Sciences, Vol. 44, No. 2, pp.121-135. http://dx.doi.org/10.1016/j.ijthermalsci.2004.07.003

Calmidi, V.V., Mahajan, R.L. (1998): Mixed convection over a heated horizontal surface in a partial enclosure, International Journal of Heat and Fluid Flow, Vol.19, pp.358-367. http://dx.doi.org/10.1016/S0142-727X(98)00002-2

Chamkha, A.J. (2002): Hydromagnetic combined convection flow in a vertical lid-driven cavity with internal heat generation or absorption, Numerical Heat Transfer, Part A, Vol. 41, No. 5, pp. 529-546. http://dx.doi.org/10.1080/104077802753570356

Garandet, J.P., Alboussiere, T., Moreau, R. (1992): Buoyancy driven convection in a rectangular enclosure with a transverse magnetic field, International Journal of Heat Mass Transfer, Vol. 35, pp. 741-748. http://dx.doi.org/10.1016/0017-9310(92)90242-K

House, J.M., Beckermann, C., Smith, T.F. (1990): Effect of a centered conducting body on natural convection heat transfer in an enclosure, Numerical Heat Transfer, Part A, Vol. 18, pp. 213–225. http://dx.doi.org/10.1080/10407789008944791

Hsu, T.H. and How, S.P. (1999): Mixed convection in an enclosure with a heat-conducting body. Acta Mechanica, Vol. 133, pp. 87-104. http://dx.doi.org/10.1007/BF01179012

Omri, A. and Nasrallah, S.B. (1999): Control Volume Finite Element Numerical Simulation of Mixed Convection in an Air-Cooled Cavity, Numerical Heat Transfer, Part A, Vol. 36, pp. 615-637.

Oztop, H.F., Zhao, Z., YU, Bo (2009): Fluid flow due to combined convection in lid-driven enclosure having a circular body, International Journal Heat Fluid Flow, Vol. 30, No. 5, pp. 886-901. http://dx.doi.org/10.1016/j.ijheatfluidflow.2009.04.009

Papanicolaou, E., Jaluria, Y. (1990): Mixed convection from an isolated heat source in a rectangular enclosure, Numerical Heat Transfer, Part A, Vol.18, pp. 427-461. http://dx.doi.org/10.1080/10407789008944802

Rahman M.M. and Alim, M.A. (2010): MHD mixed convection flow in a vertical lid-driven square enclosure including a heat conducting horizontal circular cylinder with Joule heating, Nonlinear Analysis: Modelling and Control, Vol. 15, No. 2, pp. 199–211.

Rahman, M.M., Alim, M.A., Sarker, M.M.A. (2010): Numerical study on the conjugate effect of joule heating and magneto-hydrodynamics mixed convection in an obstructed lid-driven square cavity, International Communications in Heat and Mass Transfer, Vol. 37, pp. 524-535. http://dx.doi.org/10.1016/j.icheatmasstransfer.2009.12.012

Reddy, J.N. (1993): An Introduction to Finite Element Analysis, McGraw-Hill, New-York.

Nasrin, Rehena and Parvin, Salma (2011): Hydromagnetic effect on mixed convection in a lid-driven cavity with sinusoidal corrugated bottom surface, International Communications in Heat and Mass Transfer, Vol. 38, No. 6, pp. 781-789. doi:10.1016/j.icheatmasstransfer.2011.03.002 http://dx.doi.org/10.1016/j.icheatmasstransfer.2011.03.002

Rudraiah, N., Venkatachalappa, M., Subbaraya, C.K. (1995): Combined surface tension and buoyancy-driven convection in a rectangular open cavity in the presence of magnetic field, International Journal of Non-linear Mechanics, Vol. 30 No. 5, pp. 759-770. http://dx.doi.org/10.1016/0020-7462(95)00026-K

Sivasankaran, S., Malleswaran, A., Lee, Jinho and Sundar, Pon (2011): Hydro-magnetic combined convection in a lid-driven cavity with sinusoidal boundary conditions on both sidewalls, International Journal of Heat and Mass Transfer, Vol. 54, No. 1-3, pp. 512-525. http://dx.doi.org/10.1016/j.ijheatmasstransfer.2010.09.018

Shi, W., Vafai, K. (2010): Mixed convection in an obstructed open-ended cavity, Numerical Heat Transfer; Part A: Applications, Vol. 57, No. 10, pp. 709-729. http://dx.doi.org/10.1080/10407781003800714

Shokouhmand, H. and Sayehvand, H. (2004): Numerical study of flow and heat transfer in a square driven cavity, International Journal of Engineering, Transactions A: Basics, Vol. 17, No. 3, pp. 301-317.

Zeinkiewicz, O.C., Taylor, R.L., Too, J.M. (1971): Reduced integration technique in general analysis of plates and shells, International Journal for Numerical Methods in Engineering, Vol. 3, pp. 275-290. http://dx.doi.org/10.1002/nme.1620030211